Nordic Hydrology, 21, 1990, 47-64

Radar Signal Interpretation in Warm Season Rainstorms

Nicolas R. Dalezios
Envirotech Ltd., Thessaloniki, Greece

Nicholas Kouwen
Dept. of Civ. Eng., University of Waterloo, Ont., Canada

There are several sources of error affecting the returned power of weather radar signals with an impact on the accuracy of radar rainfall measurements. In this study, several factors and sources of error are considered at the preprocessing stage of the raw radar reflectivities for surface rainfall estimation. In particular, deterministic corrective algorithms are developed and alternatively used for non-rainfall echoes, wind effect, signal attenuation and the *Z-R* relationship. These techniques are applied to a number of warm season rainstorms. A bivariate statistical objective analysis is used as a basis for comparing the different algorithms. Two error statistics are computed in order to assess the performance of each algorithm. The results indicate that the deterministic techniques constitute a necessary step in the ultimate improvement of surface rainfall estimates by weather radar.

Introduction

Precipitation is a time-space phenomenon with very high variability. Conventional raingage networks are inadequate to effectively delineate the temporal and spatial distribution of precipitating systems. It was soon realized (Hitchfield and Borden 1954) that, although radar data itself may not be fully reliable, surface rainfall estimates are improved when raingage data are used to adjust the initial radar rainfall measurements. However, the raw radar reflectivities should be processed and registered to the ground before radar rainfall measurements are conjunctively

used with raingage data as in the bivariate statistical objective analysis (Dalezios 1988a; Dalezios 1984; Dalezios and Kouwen 1983; and Dalezios 1982). At the radar data processing stage, there are several factors causing errors and affecting the accuracy of the returned power of the radar signal.

The range in reported accuracies is considerable varying with storm duration, size and type, as well as with radar range, geographical location, radar types and data processing techniques (Linsley *et al.* 1982; Wilson and Brandes 1979). Among the various sources of error, which have been described by several researchers (Battan 1973; Crozier 1975; Dalezios 1982; Linsley *et al.* 1982; Wilson and Brandes 1979) are: signal attenuation, non-uniform beam filling, variations in snow crystal type or drop size distribution, wind effect, bright band, evaporation or growth of precipitation, non-rainfall echoes, anomalous propagation, beam interception of the freezing level, frequency of radar data collection, variations in the Z-R relationship, presence of hail or other hydrometeors, errors in electronic calibration, returned power averaging errors in regions of very strong precipitation gradients and others. Some of these factors cause random errors, whereas others produce systematic bias (Zawadzki 1984) in radar rainfall measurements.

The objective of this paper consists of investigating the performance of several deterministic corrective algorithms for initial hourly radar rainfall measurements. First, data reduction and compression is exercised on the raw radar signals to generate two-dimensional radar fields for the target area. Certain deterministic corrective techniques are then applied to the radar data sets. Some preliminary results have been recently presented elsewhere (Dalezios 1988b).

In particular, two algorithms are alternatively used to correct for non-rainfall echoes: the "mask" method (Gorrie and Kouwen 1977) and the Mean-Difference (MD) algorithm (Geotis and Silver 1976). Similarly, two models are also used alternatively to take into account signal attenuation: the so-called World Meteorological Organization (WMO) model (Bigler *et al.* 1966) and an iterative corrective technique (Hildebrand 1978). Furthermore, a navigation model is applied for the wind effect on the falling precipitation (Dalezios *et al.* 1989; Dalezios and Kouwen 1983; Dalezios 1982) and different Z-R relationships are compared. The paper is organized as follows: The first section, p. 48, explains the data environment; the second section, p. 51, describes the deterministic corrective algorithms; and the third section, p. 58, discusses the results. The study is applied to the Grand River watershed above Cambridge (Galt) in southern Canada (Fig. 1).

Data Description

The data used in this study consist of surface rainfall observations from recording raingages and digitized radar reflectivities collected about every 5 minutes. A C-band (5 cm) weather radar is used, which is located at Woodbridge, Ontario, Canada (Fig. 1), the technical characteristics of which can be found in Table 1.

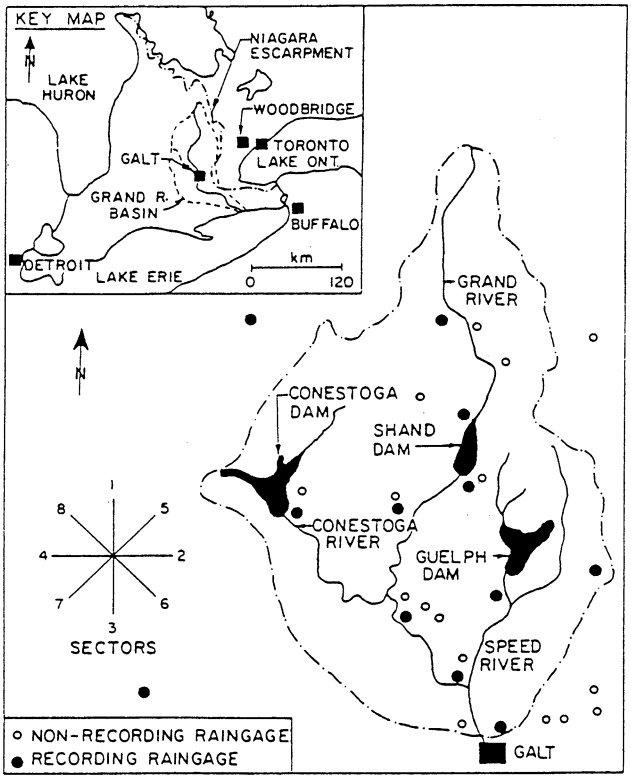

Fig. 1. The Watershed and Key Map.

Eleven warm season storm events have been selected to provide a quantitative description of rainfall patterns in the area (Table 2) and to evaluate the developed radar data preprocessing methodology. The Grand River watershed above Cambridge, 3,480 km^2 in area, has been selected for this study, which is located west of Toronto and between the 40 km and 110 km range of the radar installation. All the storms affected a large region of which the chosen watershed was only a fraction.

At the preprocessing stage, the 0.5° antenna elevation angle was selected, which is acceptable for rainfall estimates, because it reduces the effect of cross-winds, updrafts, evaporation and growth of precipitation, although at close ranges ground clutter can be a problem. For each recorded complete radar scan two-dimensional data sets are produced using a polar grid element of 2 km in range by 2° in azimuth. The bins contained within each grid element are averaged by converting the reflectivity factors to non-logarithmic units and then reconverting the average to dBz.

The next step of the process corrects for non-rainfall echoes and signal attenuation, which are described in the following section. The radar signals are then converted to rainfall rates using the so-called southern Ontario Z-R relationship (Richards and Crozier 1983) $Z = 295\ R^{1.43}$, where Z is the radar reflectivity in mm^6 / m^3 and R is the rainfall rate in mm/hr. A sensitivity analysis is conducted using two

Table 1 – Radar characteristics (from Crozier (1975)).

Parameter	Canadian FPS-101
1. Band	C
2. Frequency (MHz)	5610
3. Wavelength (cm)	5.34
4. Peak Power (Kw)	200
5. Pulse length (m)	599.6
6. Pulse duration (usec)	2.0
7. Pulse Repetition Rate (PRR) (in pps)	324
8. Vertical Beam Width (deg)	1.05
9. Horizontal Beam Width (deg)	1.10
10. Antenna (Reflector)	paraboloid
11. Reflector Diameter (ft)	12
12. Antenna Gain (db)	41.95(m)
13. Scan speed (rpm)	6.0
14. Minimum discernable Signal (MDS) (in db)	–107
15. Receiver (80 db range)	logarithmic
16. STC Normalization (nmi)	100
17. Azimuth-scan rate (rpm)	6

Table 2 – Storm characteristics

(1)	Storm (2)	Duration (hrs) (3)	Number of recording raingages (4)	Raingage network density (per km^2) (5)	Storm mean (mm) (6)
1.	18 Apr 75	13	8	1/435	35.5
2.	6 May 75	12	9	1/387	11.1
3.	18 Sep 75	20	10	1/348	24.3
4.	6 May 76	35	11	1/316	37.5
5.	5 Jul 77	6	10	1/348	13.2
6.	6 Jul 77	18	10	1/348	12.3
7.	7 Jul 77	11	10	1/348	9.6
8.	16 Aug 77	12	10	1/348	35.9
9.	10 Apr 78	28	10	1/348	47.4
10.	11 Sep 78	12	9	1/387	18.7
11.	14 Sep 78	7	8	1/435	3.0

more typical *Z-R* relationships (Jones 1956; Marshall and Palmer 1948) and the results are discussed in subsequent sections. Moreover, the radar rainfall intensity field is converted from polar to Cartesian coordinates using a 2 km × 2 km square grid element.

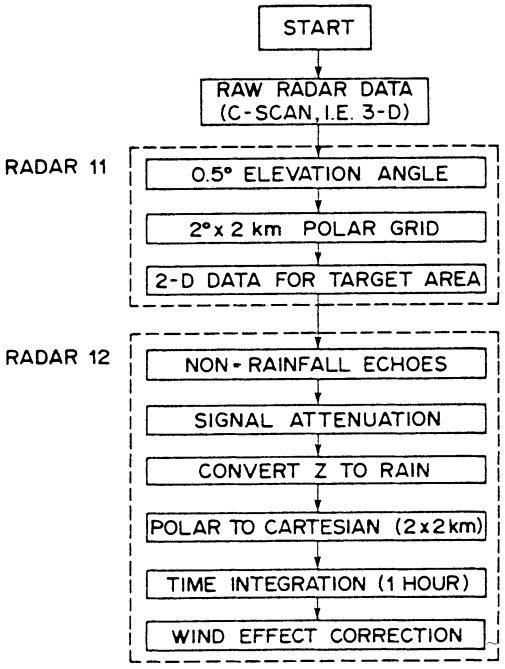

Fig. 2. The Data Preprocessing Methodology.

Since the selected integration interval (or cycle) throughout this study is one hour, time integration is applied to the intensity field over each hour to produce hourly radar rainfall fields. One hour is a common and widely used time-step or integration interval in an operational environment. One hour is long enough to permit integration of radar uncertainties associated with individual scans, to avoid fluctuations in local weather patterns and timing errors in raingage recording equipment and to overcome undetected low rainfall rates. Finally, a correction for the wind effect is applied to the radar rainfall field, which tracks the falling rainfall and registers the rainfall pattern to the ground (Dalezios and Kouwen 1983; Dalezios 1982). A flow diagram of the preliminary processing methodology is shown in Fig. 2.

Deterministic Corrective Techniques

This section provides a brief review of the theoretical and practical aspects of the deterministic corrective techniques applied to the raw radar reflectivities. Several sources of error are not considered. Beam interception of the freezing level, variations in snow crystal type and presence of other hydrometeors are ignored, since warm season storms are analysed. Similarly, errors in electronic calibration are assumed insignificant, since the radar is relatively stable over a 24-hr period

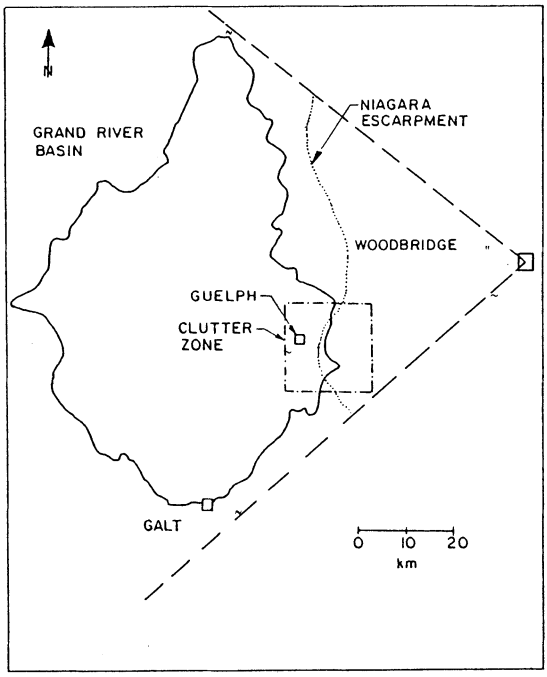

Fig. 3. Ground-Clutter Affected Area.

(Crozier 1975). Moreover, anomalous propagation is neglected, since it is rare during precipitation (Battan 1973; Crozier 1975; Wilson and Brandes 1979). Non uniform beam filling is also neglected, since the maximum radar range used is 110 km. Finally, sampling frequency at Woodbridge is a single 0.5 degree elevation scan about every five minutes, which would not introduce significant errors.

Non-Rainfall Echoes

For low elevation angles the radar beam easily intercepts natural terrain or human development. These permanent echoes can result in either partial or complete screening depending on the degree of blockage. In this study, the target area is depicted by the interference of the Niagara escarpment (Fig. 3), which has two adverse effects, namely high intensity terrain echoes, which exist over the Grand River basin just east of Guelph and partial beam blocking by the escarpment (Figs. 4 and 5).

The Mask Method – The "mask" method deals with the echo topography and the extent it affects the radar beam for various elevation angles. This technique corrects for false echoes caused by terrain interference (Gorrie and Kouwen 1977; Harrold *et al.* 1974) and can be applied to the radar signals either in real-time or in "post-facto" analyses. First, the clutter zone containing the false echoes and affecting rainfall measurements over the Grand River watershed is identified (Fig. 3).

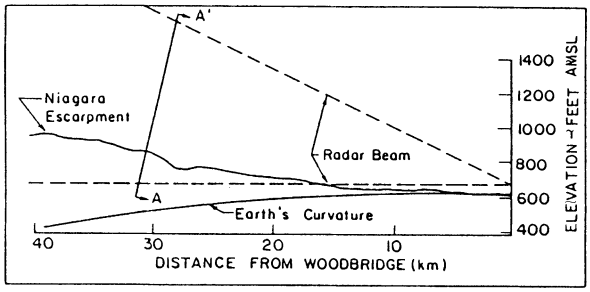

Fig. 4. The Escarpment.

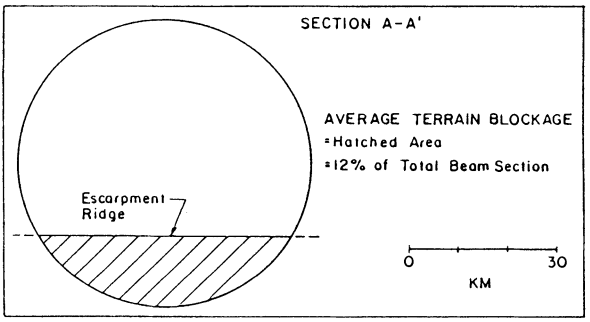

Fig. 5. The Beam Blockage.

Initially, radar measurements on 2 × 2 km Cartesian squares for clear weather were examined to determine the extent of escarpment clutter. On this basis, dry (or non-rainfall) radar reflectivities for the clutter zone are then subtracted from the corresponding grid data for measurements during rain thereby eliminating the permanent echoes. It is common practice to operate the radar for a few hours before a storm approaches the target area and select a dry hour.

The Mean-Difference (MD) Algorithm – The MD algorithm (Geotis and Silver 1976) measures the pulse-to-pulse variation of the radar signal at each sampled point using the time sequence differences in rainfall and non-rainfall echoes. In particular, the MD method measures the mean value of the difference between successive pulses over each integration cycle, *i.e.*, one hour, at each sampled or grid point. The MD method is applied to each polar grid element of 2° by 2 km over the affected area.

The MD algorithm is initially applied to a non-rainfall hour. For each grid element, the differences between successive pulses within the integration cycle are calculated. The Mean-Difference (MD) is then computed by taking the average of these differences and the cumulative frequency distribution of the MDs is computed by ranking them in ascending order and selecting a class interval, *e.g.*, 0.2 db (Fig. 6). The procedure is repeated for each rainy hour that a ground-echo rejection is desired. Fig. 7 shows a plot of the corresponding cumulative frequency

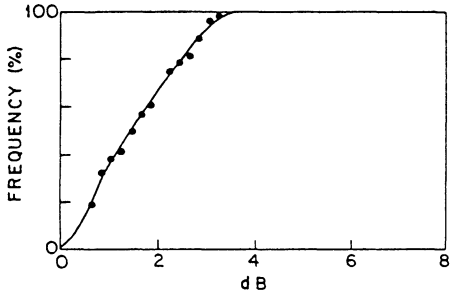

Fig. 6. Frequency Analysis: non-rainfall hour

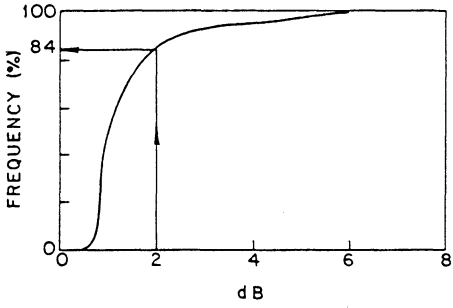

Fig. 7. Frequency Analysis: rainy hour.

distribution for a sample rainy hour. A threshold value, *e.g.*, 2 db, is then selected from Fig. 7, where the percentage of rejected rainfall is essentially small. Finally, using the selected threshold, the percentage of ground echo to be rejected is found (Fig. 6) and the radar data within the affected area are adjusted accordingly.

Signal Attenuation

The decrease in the received signal power is known as attenuation. The equation

$$\sigma_c \cong \frac{\pi^5 |K|^2 D^6}{\lambda^4} \qquad (1)$$

relates the back scatter cross-section σ_c to particle diameter D, dielectric constant $|K|^2$ and the wavelength λ. In a general form the attenuation factor K can be defined as

$$10 \log K \equiv 2 \int_0^r (g+c+p)\, dr \qquad (2)$$

where g, c and p are the one-way attenuation in db/km by gases, cloud and precipitation, respectively, and r is the radar range (Dalezios and Kouwen 1983). For a C-band (5cm) radar, gases and cloud droplets can be easily neglected, whereas

attenuation by precipitation size hydrometeors can have a significant effect in cases of intense rainfall, since it depends on wavelength, temperature, liquid water content and drop-size distribution, which is relatated to terminal velocity and rainfall intensity.

The WMO Model – In a comprehensive report (Bigler *et al.* 1966) the average two-way attenuation due to precipitation in db/km is determined based on a mean drop-size distribution in rain ad the corresponding rainfall rate. The report provides results in a tabular form showing attenuation values at different rainfall rates and for different wavelengths. Using these data, a functional relationship is developed for a *C*-band radar in the form of the following power law

$$K(r) \equiv 4.35\, R(r)^{1.17} \tag{3}$$

where $K(r)$ is the attenuation factor in db/km at range r and $R(r)$ is the rainfall rate in mm/hr at range r. Eq. (3) is used to calculate the attenuation factor and to adjust the rainfall rates on the polar grid elements, accordingly.

The Iterative Corrective Technique – This iterative algorithm has been adopted from Hildebrand's attenuation correction scheme (Hildebrand 1978). Starting with the Ontario Z-R relationship $Z = 295\, R^{1.43}$ (Richards and Crozier 1983), which relates the attenuated reflectivity factor $Z_1(r)$ at range r and the attenuated rainfall rate $R_1(r)$, an estimate of the attenuation factor $K_1(r)$ due to rain is obtained given by the following equation (Marshall and Palmer 1948)

$$K_1(r) \equiv \int_0^r KR^a\, dr \tag{4}$$

where K_1 is expressed in db, R is the rainfall rate in mm/hr and K and a are empirical coefficients. The term $K R^a$ of Eq. (4) is equivalent to the term p of Eq. (2). For warm season storms, the values of $K = 0.0047$ and $a = 1.1$ are used (Geotis and Silver 1976), which correspond to 5.7 cm wavelength and water at 18° C. The attenuation factor $K_1(r)$ is then used in the following equation

$$\log Z_2(r) \equiv \log Z_1(r) + 2 \sum_{n=1}^{r-1} K_1(n) \tag{5}$$

where $Z_2(r)$ is the new estimate of the reflectivity factor at range r. Furthermore, these new estimates are again used through the Z-R relationship and Eq. (4) to calculate new attenuation factors $K_2(r)$ and the procedure is repeated until the change in the term

$$2 \sum_{n=1}^{r_{max}} K_2(n)$$

is less than 1 db from the previous iteration. This iterative algorithm is applied radially to each polar grid element.

Wind Effect

Wind can have two adverse effects on the falling precipitation both causing errors: the vertical motion, which can be either updraft or downdraft and the horizontal drift. For the vertical wind motion, raingages can be used to calibrate and adjust the radar reflectivities (Collier *et al.* 1983; Harrold *et al.* 1974). Since the objective of this paper consists of providing initial estimates of surface rainfall, only the horizontal drift is examined, *i.e.,* the horizontal displacement between radar rainfall echoes and rainfall patterns received on the ground. For an inclined radar beam the horizontal drift of rainfall due to cross winds is range dependent and for real-time or near real-time applications in small areas or watersheds the problem can become acute.

In this paper, a deterministic wind navigation or advection model is employed (Dalezios *et al.* 1990; Dalezios and Kouwen 1983; Dalezios 1982). This model uses kinematic equations to extrapolate the precipitation field from the level it is detected by radar to the ground and its development is based on the following assumptions: the level at which radar detects precipitation is near and below the gradient level of the planetary boundary layer where the falling particle has already reached its terminal velocity with a fallspeed of 5 m/s; the trajectory of the falling particle is assumed parabolic in the Ekman layer and logarithmic in the surface layer; the wind direction is assumed constant with height in the Ekman layer; the vertical wind shear is assumed constant in the Ekman layer; and the wind field is homogeneous over the target area.

In the Ekman layer and for the assumed constant vertical wind shear, the kinematic equations of a falling particle are represented by the following system

$$\frac{dz_1}{dt} = V_d \tag{6}$$

and

$$\frac{dx_1}{dt} = a_0 + az_1 \tag{7}$$

where V_d is the terminal velocity of the falling particle, and a_o and a are the intercept and the slope of the linear wind profile, respectively, yielding the following equation

$$z_1(t) = V_d t + z_{01} \tag{8}$$

where the constant of integration z_{01} is the height of the gradient level. Eqs. (7) and (8) yield the parabolic particle trajectory

$$x_1(t) = \frac{aV_d}{2} t^2 + (a_0 + az_{01})\, t \tag{9}$$

where $x_1(t)$ is the horizontal displacement of the falling particle at time t relative to axes fixed at the ground.

In the surface layer the wind profile can be expressed by

$$\frac{\theta \bar{u}}{\theta x} = \frac{u_w}{l_x} \tag{10}$$

where u is the mean wind velocity, l_x is the mean mixing length and u_w is the friction velocity or dynamic velocity defined by the identity $u_w^2 \equiv \tau_o/p$, where τ_o is the surface stress and p is the density, both assumed constant with height. Integrating Eq. (10) with respect to z yields the logarithmic wind profile

$$u = \frac{u_w}{K} \ln\left(\frac{z}{z_0}\right) \quad , \quad z \geq z_0 \tag{11}$$

where the constant of integration z_o, called the roughness parameter, is selected so that $u = 0$ at $z = z_o$. Since it is assumed that the x-axis is parallel to the wind flow and has a logarithmic profile (Eq. (11)), the kinematic equations of the surface layer are

$$\frac{dz_2}{dt} = V_d \tag{12}$$

and

$$\frac{dx_2}{dt} = s \ln\left(\frac{z}{z_0}\right) \tag{13}$$

where s is the slope of the regression line given by $s = u_w/K$. Integrating the above equations with respect to time produces the following results

$$z_2(t) = V_d t + z_{02} \tag{14}$$

and

$$x_2(t) = -s(1 + \ln z_0)\, t + \frac{s(z_{02} + V_d t)}{V_d} \ln(z_{02} + V_d t) - \frac{s z_{02}}{V_d} \ln z_{02} \tag{15}$$

where z_{o2} is the top of the surface layer.

The horizontal wind is estimated from information on the storm motion. The model also finds the time required for a particle to reach the ground from the level it is detected by radar. Since the wind field is assumed to be homogeneous over the target area, the entire radar-rainfall field is shifted to one of the eight wind directions according to the estimated displacement.

Z-R Relationship

An empirical relationship exists between the radar reflectivity factor Z and the rainfall rate R. The expression, which explains the characteristics of precipitation, is often referred to as the Z-R relationship and is given by

$$Z = a R^b = \sum \left(\frac{D}{2}\right)^6 \tag{16}$$

where Z is expressed in mm^6 / m^3, R is in mm/hr, $D/2$ is the raindrop radius in mm, and a and b are empirical coefficients. Since the reflectivity factor Z depends on the sixth power of the drop diameter, the Z-R relationship depends sensitively on the nature of the rain drop-size distribution and shows large variations between geographical areas, between storms, as well as within storms. The choice of the proper Z-R relationship may have an impact on the accuracy of radar-rainfall estimates.

There have been many studies of the Z-R relationship (Battan 1973; Crozier 1975; Marshall and Palmer 1948; Richards and Crozier 1983; Stout and Mueller 1968) and there are almost as many Z-R relationships as there are studies. For example, it has been found that the constant "a" in the Z-R relation varies from 140 for drizzle, through 250 for widespread rain to 500 for thunderstorm rain. Three different Z-R relationships are used and compared in this study: the Marshall-Palmer relationship (Marshall and Palmer 1948), also known as the "climatological" relationship with $a = 200$ and $b = 1.6$; the southern Ontario Z-R relationship (Richards and Crozier 1983) with $a = 295$ and $b = 1.43$; and the Illinois Z-R relationship (Jones 1956) with $a = 485$ and $b = 1.37$.

Results and Discussion

Eleven warm season storms (Table 2) have been selected to demonstrate the efficiency of the corrective techniques on point as well as on areal radar rainfall measurements and the results are presented in Tables 3, 4, and 5. In this study, a bivariate statistical objective analysis conjunctively using raingage and radar data sets is employed to generate hourly surface rainfall fields, which is described in detail elsewhere (Dalezios 1988a; Dalezios 1984; Dalezios and Kouwen 1982; Dalezios 1982). Two error statistics are employed, namely the Mean Storm Radar Bias (MSRB) and the Mean Absolute Percentage Difference (MAPD). The MSRB or the average G/R ratio is used to evaluate the accuracy of point rainfall measurements in the employment of individual deterministic corrective techniques and is expressed as

$$MSRB = \frac{1}{N} \sum_{i=1}^{N} \left(\frac{G}{R}\right)_i \tag{17}$$

where G is the observed rainfall for raingage i, R is the 6 km × 6 km spatially averaged radar rainfall estimate around raingage i and N is the number of record-

ing raingages used in the analysis. For a perfect analysis the bias should be equal to one.

Similarly, the MAPD attempts to evaluate the effect of the individual deterministic corrections on the storm average areal rainfall. The MAPD takes the form

$$MAPD \equiv 100 \frac{|R_a - R_u|}{R_a} \tag{18}$$

where R_a refers to the storm areal radar rainfall estimate obtained by using the bivariate statistical objective analysis and the corresponding corrective algorithm, whereas R_u is the storm areal radar rainfall estimate by using the bivariate objective analysis. In the present study, a simple statistical validation method is used, which divides the existing raingage stations into a calibration network and a test network. The calibration network consists of the recording raingages (Fig. 1) used in the analysis to estimate point rainfall values at every sampling location of a test network of the non-recording raingages (Fig. 1).

Tables 3 and 4 present the effect of the individual corrective techniques on the accuracy of point and areal radar rainfall measurements, respectively, using the calibration raingage network. The results confirm previous findings that, in general, radar tends to overestimate light, widespread and long-duration rainfall and to underestimate moderate and heavy rainfall of convective nature (Wilson and Brandes 1979). Furthermore, spatial smoothing in the raw radar data and time integration introduces bias and scatter in comparisons of radar and raingage data.

With respect to the effect of the correction for non-rainfall echoes on point rainfall measurements, the two techniques show similar performance (Table 3). However, both techniques show the same variations in the MSRB values for non-rainfall echoes of Table 3 mainly related to the type of storm. In particular, the MSRB values for light to moderate storms with relatively short duration (Table 2) are close to unity, whereas for heavy storms with uneven distribution the MSRB values are relatively higher justifying, thus, the above mentioned underestimation of radar rainfall. Moreover, there is a difference in the performance of the two techniques for non-rainfall echoes in areal storm rainfall (Table 4). In the MD method, the time step of one hour used throughout this study was not long enough to allow for the selection of a satisfactory threshold value and the desired percentage of ground echo was not rejected in several cases.

Similarly, with respect to signal attenuation on point radar rainfall measurements (Table 3) the two techniques indicate the same performance, whereas in areal storm rainfall there is a difference in the performance of the two techniques (Table 4). It should be mentioned that Table 3 shows the same storm-to-storm variation for signal attenuation as for non-rainfall echoes. However, Table 4 indicates that a within storm investigation is needed to expose the hourly fluctuations in signal attenuation, especially in high rainfall intensities for a precise evaluation of the alternatively used algorithms.

Table 3 – The computed mean storm radar bias (MSRB) of individual corrective Techniques.

Storm		Corrective techniques							
		Non-rainfall echoes (Two Methods)		Signal attenuation (Two Methods)		Wind effect	*Z-R* relationship (Three Equations)		
		Mask Method	MD Method	WMO Model	Iter. Model	Navig. Model	a=200 b=1.6	a=295 b=1.43	a=485 b=1.37
(1)	(2)	(3)	(4)	(5)	(6)	(7)	(8)	(9)	(10)
1.	18 Apr 75	3.95	4.02	3.65	3.57	3.53	1.18	1.28	1.20
2.	6 May 75	2.55	2.78	2.31	2.20	2.41	1.31	1.29	1.49
3.	18 Sep 75	2.01	2.23	1.90	1.84	1.89	1.01	1.10	1.16
4.	6 May 76	1.20	2.24	1.85	1.79	1.86	1.01	1.05	1.06
5.	5 Jul 77	1.45	1.59	1.45	1.45	1.46	0.91	0.82	0.95
6.	6 Jul 77	0.58	0.60	0.57	0.57	0.57	0.75	0.74	0.75
7.	7 Jul 77	1.11	1.21	1.09	1.08	1.08	0.75	0.74	0.75
8.	16 Aug 77	2.24	2.52	2.12	2.11	2.10	1.18	0.90	1.20
9.	10 Apr 78	3.27	3.49	3.26	3.17	3.40	1.57	1.55	1.63
10.	11 Sept 78	1.64	1.77	1.64	1.59	1.62	1.00	1.02	1.08
11.	14 Sep 78	0.39	0.41	0.39	0.38	0.38	0.34	0.35	0.36
Average		1.93	2.08	1.84	1.80	1.85	0.97	0.98	1.03

Note: the calibration raingage network was used.

Moreover, Tables 3 and 4 show the results of the wind effect on the accuracy of radar rainfall measurements. The results indicate that the average horizontal displacement is about 2.5 km. This finding shows a minor effect on hourly surface rainfall estimates, which is expected since the analysed warm season storms were major storms with sizeable areal coverage and long duration (Table 2). They also show that, on the average, two minutes are approximately necessary for the rain particles to fall to the ground from the level they are detected by radar, since radar detects rain particles at the centroid of the selected watershed (Fig. 2) at a height of about 620 m. This is not crucial for time steps of the order of one hour or longer and for areas for the selected size. However, for time steps of one or two minutes this correction may prove to be essential. Moreover, for small areas the problem can become acute, since the wind effect can have a significant impact on the mean areal rainfall.

Furthermore, the choice of the proper *Z-R* relationship may have an effect on the accuracy of radar rainfall estimates. It is well known that the *Z-R* relationship shows, in general, a very high temporal and spatial variability between geographical regions, between storms, as well as within storms. The results of the three *Z-R* relations are presented in columns (8) to (10) of Table 3. Needless to say, the Marshall-Palmer relationship is a well accepted model and widely used. However, the MSRB of the calibration network shows similar performance for the three relationships. In fact, the overall average values of the three *Z-R* relationships are

Table 4 – The computed mean absolute percentage difference (MAPD) (%) of individual corrective techniques.

	Storm	Corrective techniques				
		Non-rainfall echoes (Two Methods)		Signal attenuation (Two Methods)		Wind effect
		Mask Method (%)	MD Method (%)	WMO Model (%)	Iter. Model (%)	Navig. Model (%)
(1)	(2)	(3)	(4)	(5)	(6)	(7)
1.	18 Apr 75	2.00	21.3	1.00	14.7	5.2
2.	6 May 75	0.50	17.8	1.00	14.2	4.5
3.	18 Sep 75	2.90	30.7	1.00	15.7	9.9
4.	6 May 76	1.90	22.6	1.10	17.8	6.4
5.	5 Jul 77	0.60	13.2	0.60	2.7	2.1
6.	6 Jul 77	0.50	12.0	0.70	2.3	2.7
7.	7 Jul 77	0.80	18.0	0.90	7.6	3.9
8.	16 Aug 77	1.70	23.0	0.70	4.9	4.0
9.	10 Apr 78	1.60	20.2	1.00	16.9	5.0
10.	11 Sep 78	1.50	16.9	1.00	6.7	3.1
11.	14 Sep 78	0.80	16.1	1.10	5.5	1.5
Average		1.35	19.2	0.92	9.91	4.39

Note: The calibration raingage network was used.

all close to one and very close to each other. Thus the similarity in the results allows the use of the southern Ontarion *Z-R* relationship in this study with confidence.

Finally, Table 5 shows the effect of all three sources of error on the total storm average areal rainfall for the bivariate statistical objective analysis using the independent test network of five storms, since non-recording raingage data was available only for these storms. It should be mentioned that the use of the independent test raingage network justifies the socalled pure validation procedure, as opposed to the cross validation procedure when the calibration network is used. As a correction for non-rainfall echoes the Mean-Difference algorithm is considered, whereas for signal attenuation the iterative corrective technique.

For the calculation of the MAPD of column (3) in Table 5 the unadjusted mean areal rainfall *Ru* is computed by using the bivariate objective analysis (Dalezios 1988a; Dalezios 1984; Dalezios 1982), whereas the adjusted mean areal rainfall *Ra* is computed by using the bivariate statistical objective analysis and the three deterministic algorithms. Similarly, for the computation of the MAPD of column (4), *Ru* refers to the unadjusted storm total mean areal radar rainfall estimate by simply converting reflectivities to rainfall rates using the southern Ontario *Z-R* relationship, and *Ra* is the storm total mean areal radar rainfall estimate as adjusted by the three deterministic corrective techniques.

Table 5 – The effect of all three corrective techniques in the mean areal precipitation.

	Storm	Mean Absolute Percentage Difference (MAPD)	
		with bivariate analysis (%)	without bivariate analysis (%)
(1)	(2)	(3)	(4)
1.	18 Apr 75	6.63	2.07
2.	18 Sep 75	17.69	13.95
3.	6 May 76	8.26	0.10
4.	16 Aug 77	2.10	19.57
5.	10 Apr 78	1.31	2.15
Average		7.2	7.57

Note: The test raingage network was used.

The results of Table 5 using the independent test raingage network indicate that the overall average MAPD values of columns (3) and (4) are 7.2%, and 7.57%, respectively. These average MAPD values demonstrate the effect of the three selected deterministic algorithms and justify their need on storm areal radar rainfall estimates with or without the employment of the bivariate statistical objective analysis. As expected, these average MAPD values are close to each other. Needless to say, the MAPD is an independent and objective criterion. However, the MAPD is not an indication of the average percentage error, but rather it resembles the root mean square error (*rms*). Notice that the MAPD can have a high value, while the mean percentage error can be close to zero.

Summary and Conclusions

A number of deterministic corrective techniques have been developed and alternatively used to consider non-rainfall echoes, signal attenuation, wind effect and Z-R relationship in radar rainfall measurements. Two commonly used statistics have been employed to assess the performance of the developed deterministic algorithms on point, as well as on areal rainfall estimates. The results show that objective surface rainfall estimation analyses such as the bivariate objective analysis, which incorporates radar and raingage data sets, is affected by several sources of error. There are differences in the performance of the alternatively used corrective algorithms as inferred from the two employed statistics. It is mainly the MAPD (Table 4), which shows differences in the alternative use of the deterministic techniques for storm areal rainfall estimation, whereas the MSRB (Table 3) is not very indicative of variations in the performance of different algorithms on point rainfall estimation.

Deterministic corrective techniques are still necessary for the ultimate improvement of surface rainfall estimates. The selection of the proper *Z-R* relationship does not have a significant impact on the analysis. The sourthern Ontario *Z-R* relationship, which has been used throughout this study, gives satisfactory results. The classic Marshall-Palmer *Z-R* relationship performs equally well.

Acknowledgements

This study was supported by the Natural Sciences and Engineering Research Council (NSERC) of Canada and by the Provincial Government of Ontario through an Ontario Graduate Scholarship (OGS). The authors are grateful to Mr. C. L. Crozier of the Atmospheric Environment Service (AES), Environment Canada, for useful discussions and providing the necessary data.

References

Battan, L.J. (1973) *Radar Observations of the Atmosphere,* The University of Chicago Press, 324 p.

Bigler, S.G., *et al.* (1966) Use of Ground-Based Radar in Meteorology, Tech. Note No. 78, WMO-No. 193.

Collier, C.G., Larke, P.R., and May, B.R. (1983) A Weather Radar correction procedure for real-time estimation of surface rainfall, *Q.J.R. Meteor. Soc., Vol. 109*, pp. 589-608.

Crozier, C.L. (1975) A C-Band Meteorological Radar System for Quantitative Measurement and Cloud Physics Research, Atm. Env. Service, Meteor. Memoirs, N. 30.

Dalezios, N.R., Kouwen, N., and Linardis, P.C. (1990) Modeling and Navigating Space-Time Drift of Digitized Radar Rainfall Patterns, *Intern. J. of Remote Sensing* (in press).

Dalezios, N.R. (1988a) Objective Rainfall Evaluation in Radar Hydrology, *J. Water Res. Plan. Man. Div. (JWRMD5), ASCE, Vol. 114(5),* pp. 531-546.

Dalezios, N.R. (1988b) Digital Processing of Weather Radar Signals for Rainfall Estimation. Submitted and presented at the Intern. Conference on Advances in Remote Sensing, Aristotle Univ. of Thessaloniki Greece, October.

Dalezios, N.R. (1984) On the Accuracy of Rainfall Measurements by Weather Radar, Proceedings, 9th Can. Symp. on Remote Sensing, CRSS, pp. 309-315.

Dalezios, N.R., and Kouwen, N. (1983) On the Registration of the Radar Rainfall Field to the Ground, Proceedings, 8th Can. Symp. on Remote Sensing, CRSS, pp. 195-204.

Dalezios, N.R., and Kouwen, N. (1982) On the Structure of Homogeneous Anisotropic Correlation Functions for Real-Time Radar Rainfall Estimation, in *Hydrometeorology,* edited by Johnson and Clark, AWRA, pp 153-157.

Dalezios, N.R. (1982) Real-Time Radar Rainfall Measurements for Hydrologic Modeling. Ph.D. thesis, University of Waterloo, Waterloo, Ontario, Canada, 210p.

Geotis, S.G., and Silver, W.M. (1976) An Evaluation of Techniques for Automatic Ground-Echo Rejection. Preprints, 17th Conf. on Radar Meteor., Oct. 26-29, Seattle, AMS, pp. 448-452.

Gorrie, J.E., and Kouwen, N. (1977) Hydrological Applications of Calibrated Radar Precipitation Measurements. Preprints, 2nd Conf. on Hydrometeorology, Toronto, Oct. 25-27, AMS, pp. 272-279.

Harrold, T.W., English, E.J., and Nicholass, C.A. (1974) The Accuracy of Radar Derived Rainfall Measurements in Hilly Terrain, *Q.J.R. Meteor. Soc., Vol. 100,* pp. 331-350.

Hildebrand, P.H. (1978) Iterative Correction for Attenuation of 5 cm Radar in Rain, *JAM, Vol. 17,* pp. 508-514.

Hitchfield, W., and Borden, J. (1954) Efforts Inherent in the Radar Measurement of Rainfall at Attenuating Wavelengths, *JAM, Vol. 11,* pp. 58-67.

Jones, D.M.A. (1956) Rainfall Drop-Size Distribution and Radar Refelctivity, Res. Rept. No. 6, Ill. State Water Survey.

Linsley, R.K., Kohler, M.A., and Paulhus, J.L.H. (1982) *Hydrology for Engineers,* McGraw-Hill, 3rd Edition.

Marshall, J.S., and Palmer, W.M. (1948) The Distribution of Raindrops with Size, *JAM, Vol. 5*, pp. 165-166.

Richards W.G., and Crozier, C.L. (1983) Precipitation Measurement with a C-Band Weather Radar in Southern Ontario, *Atm.-Ocean Vol. 21(2),* pp. 125-137.

Stout, G.E., and Mueller, E.A. (1968) Survey of Relationships between Rainfall Rate and Radar Reflectivity in the Measurement of Precipitation, *JAM, Vol. 7,* pp. 465-474.

Wilson, J.W., and Brandes, E.A. (1979) Radar Measurement of Rainfall - A Summary, *Bull. AMS, Vol. 60(9),* pp. 1048-1058.

Zawadzki, I.I. (1984) Factors Affecting the Precision of Radar Measurements of Rain. Preprints, 22nd Conf. on Radar Meteor., Zurich, Switz., AMS, pp. 251-256.

Received: 5 April, 1989
Revised version received: 15 November, 1989
Accepted: 16 November, 1989

Address:
Nicolas R. Dalezios,
ENVIROTECH Ltd.,
132 Olympou Street,
54635 Thessaloniki,
Greece.

Nicholas Kouwen,
Department of Civil Engineering,
University of Waterloo,
Waterloo Ontario,
Canada N2L 3G1.